Cortical distance determines whether flankers cause crowding or the tilt illusion

Isabelle Mareschal Department of Optometry and Visual Science, City University, London, UK

Michael J. Morgan Department of Optometry and Visual Science, City University, London, UK

Joshua A. Solomon Department of Optometry and Visual Science, City University, London, UK

Differences between target and flanker orientations become exaggerated in the tilt illusion. However, small differences sometimes go unnoticed. This small-angle assimilation shares many similarities with other types of visual crowding but is typically found only with small and/or hard-to-see stimuli. In Experiment 1, we investigated the effect of stimulus visibility on orientation bias using relatively large stimuli. The introduction of visual noise increased the perceived similarity of target and flanker orientations at retinal eccentricities of 4° and 10°; however, small-angle assimilation was found only at 10°. The effects of eccentricity were reduced in Experiment 2, when our stimuli were "M-scaled" for equal cortical coverage. Further support for a cortical substrate was obtained in Experiment 3, in which the effects of target–flanker separation were measured. When biases from all three experiments are expressed as a fraction of the inducing flankers' angle, and plotted as a function of the approximate cortical separation between the target and its closest flanker, they form a curve like the cross-section of half a Mexican hat. We conclude that the tilt illusion and small-angle assimilation reflect opponent influences on orientation perception. The strength of each influence increases with cortical proximity and stimulus visibility, but the one responsible for assimilation has a lesser extent.

Keywords: detection/discrimination, spatial vision, space and scene perception

Citation: Mareschal, I., Morgan, M. J., & Solomon, J. A. (2010). Cortical distance determines whether flankers cause crowding or the tilt illusion. *Journal of Vision, 10*(8):13, 1–14, http://www.journalofvision.org/content/10/8/13, doi:10.1167/10.8.13.

Introduction

Context has long been known to influence the appearance of individual items in the visual field. For example, when asked to determine whether a particular item is tilted clockwise or anti-clockwise of vertical, observers' responses can be biased by the tilt of neighboring items. Several studies have confirmed this tilt illusion, originally reported by Gibson (1937). In one such study (Solomon, Felisberti, & Morgan, 2004), a Gabor "target" required approximately 4° of tilt to be reported clockwise and anti-clockwise with equal frequency, when presented at 3.7° eccentricity and flanked by Gabors tilted 22° or 45° in the same direction.

However, when Solomon et al. (2004) used 5° tilted flankers, they found something qualitatively different: these slightly tilted flankers did not repel the target, they attracted it. A similar result was reported by Kapadia, Westheimer, and Gilbert (2000), who used small line segments in the center of the visual field. Their results were qualitatively similar to those of Solomon et al.; assimilation changing to repulsion, as the flankers became increasingly oblique.

Small-angle assimilation makes targets look more like their flankers. It therefore hampers attempts to discriminate between otherwise identical targets having slightly different orientations. Consequently, we can expect the acuity loss known as "crowding" (Stuart & Burian, 1962) wherever we find small-angle assimilation.[1]

The disparity in documentary evidence suggests that small-angle assimilation is much less robust than the tilt illusion. In fact, Solomon and Morgan (2006) showed that small-angle assimilation is absent when a large, center–surround configuration is used at fixation. Thus, we can add Gabor patterns to the list of visual targets, including Landolt rings (Jacobs, 1979) and Vernier lines (Levi, Klein, & Aitsebaomo, 1985) that remain resistant to crowding at fixation.

The (parafoveal) eccentricity of 3.7° used by Solomon et al. (2004) may have favored small-angle assimilation, but parafoveal eccentricities (e.g., 7°) have also been found to amplify the tilt illusion (Over, Broerse, & Crassini, 1972). Another possibility is that it was the unusually low visibility of stimuli in the studies by Kapadia et al. (2000) and Solomon et al. (2004), which facilitated small-angle assimilation.

doi: 10.1167/10.8.13 Received December 17, 2009; published July 21, 2010 ISSN 1534-7362

Experiment 1 (below) describes a test of this latter hypothesis. We measured orientation biases at three different retinal eccentricities (0, 4, and 10°) and two different visibilities. Visibility was manipulated by adding a random texture (i.e., luminance noise) to the target and its flankers. Experiment 2 was similar, except we attempted to disentangle the independent variables of eccentricity and cortical coverage by using "M-scaled" stimuli (i.e., Duncan & Boynton, 2003; Motter & Simoni, 2007; Rovamo & Virsu, 1984). Experiment 3 was also similar, except that the retinal separation between target and flankers was varied without varying their retinal sizes.

Note that orientation biases are necessarily either assimilative (i.e., an untilted target appears tilted in the same direction as the flankers) or repulsive (i.e., it appears tilted in the opposite direction). If assimilation and repulsion reflect opponent influences on orientation perception, then our results have direct implications for their spatial extents. These matters will be addressed in the Discussion section.

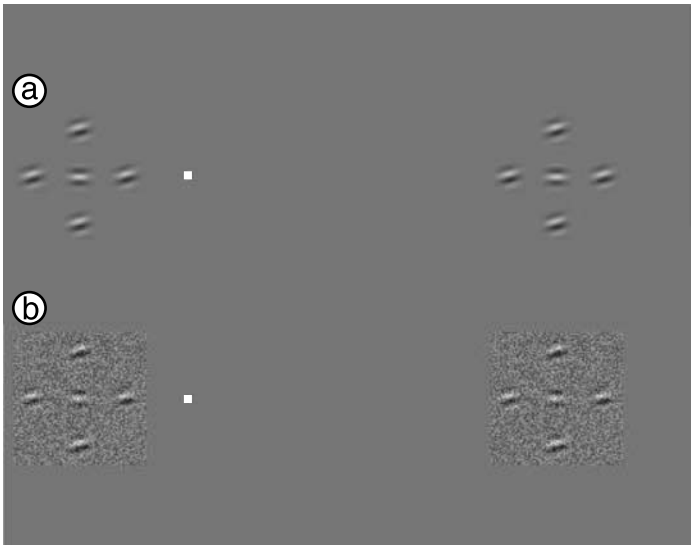

Figure 1. Sample stimulus configuration used in Experiment 1 (unscaled). Note that only one stimulus was presented at a time, either to the left or right of fixation. (a) By fixating the white dot, the target in the stimulus on the left should appear tilted clockwise of horizontal (repulsion) whereas the target on the right should appear like the flankers, tilted slightly anti-clockwise of horizontal (crowding). (b) The strength of repulsion is weakened in noise.

Methods

Observers

One of the authors (IM) and five naive observers served as subjects. All wore optical correction as necessary.

Apparatus and stimuli

An Apple Macintosh G4 computer running Matlab (MathWorks) was used for stimulus generation, experiment control, and recording subjects' responses. The programs controlling the experiment incorporated elements of the PsychToolbox (Brainard, 1997). Stimuli were displayed on a Value Vision monitor (resolution: 1280 × 1024 pixels, refresh rate: 60 Hz) driven by the computer's built-in graphics card. We achieved true 14-bit contrast resolution in grayscale using a Bits++ system (Cambridge Research Systems). The display was calibrated using a photometer and linearized using look-up tables in software. At the viewing distance of 57 cm, one pixel subtended 2.1 arcmin.

Experiment 1: Unscaled stimuli

Examples of the stimuli are shown in Figure 1. Each Gabor pattern was presented at 40% of the maximum contrast. It was the product of a sinusoidal luminance grating (1.78 c/deg) and a circular Gaussian window (where the standard deviation σ equals 0.28°) centered on a white stripe. The center-to-center spacing of the target with each flanker was 1.75°. All four flankers had the same tilt with respect to horizontal. It was selected at random from the set {−22°, −10°, −5°, 5°, 10°, 22°}, where negative angles indicate anti-clockwise tilts. When noise was present, it was added to the target and flankers. Each of its 192 × 192 pixels was drawn from a normal distribution, fixed at 32% r.m.s. contrast. To discourage eye movements, the target, flankers, and noise (when present) were displayed simultaneously for 170 ms. In the Peripheral conditions, these stimuli appeared randomly on the left or right, 10° of visual angle away from fixation. In the parafoveal conditions, the retinal eccentricity was 4°, and in the foveal conditions, it was 0. There were six conditions in total: three retinal eccentricities with noise and the same eccentricities without noise. Different flanker tilts were randomly interleaved in blocks of 240 trials within each condition.

Experiment 2: Scaled stimuli

Because less cortex is devoted to more peripheral stimuli (e.g., Fritsches & Rosa, 1996), retinal eccentricity and cortical coverage were confounded in Experiment 1. Experiment 2 reflects our attempt to tease apart these variables. We used larger stimuli at the larger eccentricities. The specific relationship between eccentricity and

stimulus size was determined using the following equation by Duncan and Boynton (2003; see also Motter & Simoni, 2007):

$$1/M(w) = 0.065w + 0.054, \quad (1)$$

where w is eccentricity in degrees, and $M(w)$ is the cortical magnification factor as a function of eccentricity. Note that with this scaling procedure, spatial frequency as well as size changes with eccentricity, but bandwidth remains constant. We opted to at least approximately equate Experiment 2's parafoveal stimuli with those of Experiment 1. Thus, for all stimuli, we used a center-to-center spacing of 3.5λ, where λ denotes the wavelength of the grating. In the non-foveal conditions, the viewing distance remained 57 cm, but the fixation point was moved 3 cm from the left edge of the monitor, and the stimuli were only presented to the right of fixation. At 4° eccentricity, target and flankers had a spatial frequency of 1.96 c/deg. Their Gaussian windows had a standard deviation of 0.25°. Target–flanker separation was 1.8°. For the stimuli presented at 10° eccentricity, M-scaling resulted in a spatial frequency of 0.94 c/deg, Gaussian windows with standard deviation of 0.53°, and a target–flanker separation of 3.84°. To obtain the requisite spatial frequency at the fovea, we had to increase the viewing distance to 192 cm. This resulted in a spatial frequency of 12 c/deg, Gaussian windows with a standard deviation of 0.04°, and a target–flanker separation of 0.29°.

Experiment 3: Spacing

The stimuli used in Experiment 3 were identical to the no-noise parafoveal and peripheral stimuli used in Experiment 1, except that additional center-to-center spacings were used in these two conditions. When the target was presented at 4° eccentricity, its flanks were centered 1.19° and 1.58° away. Much smaller spacings would have been impossible without visible overlap between the target and its flankers. When the target was presented at 10° eccentricity, its flanks were centered 2.38°, 3.17°, and 4.36° away.

Procedure

Observers fixated a small white square (2 pixels × 2 pixels) that was present throughout stimulus presentation, except in the foveal conditions where it was only present prior to stimulus presentation. Target tilts (with respect to horizontal) were drawn with equal frequency from the set: {−20°, −10°, −5°, −3°, −2°, −1°, 1°, 2°, 3°, 5°, 10°, 20°}. In the peripheral conditions, target tilts of ±50° were also tested. The observers' task was to indicate with a key-press whether the target was tilted clockwise or counter-clockwise of horizontal. For each flanker orientation tested, observers completed a minimum of 720 trials in blocks of 240.

Results

From each block of trials, six psychometric functions were obtained (one for each flanker tilt). Estimates of orientation bias and threshold (i.e., the just noticeable tilt) were derived by fitting a two-parameter cumulative Gaussian distribution of target tilt θ to the proportion of clockwise responses:

$$P(\text{“}CW\text{”}|\theta) = \frac{1}{\sqrt{2\pi}\sigma}\int_{-\infty}^{\theta} e^{-\frac{(u-\mu)^2}{2\sigma^2}}du. \quad (2)$$

Bias is the opposite of this distribution's mean $-\mu$, and threshold is its standard deviation σ (Solomon et al., 2004). In this paper, we discuss only biases.

The low occurrence of errors (i.e., clockwise responses to targets tilted anti-clockwise of horizontal and vice versa) with the most extreme target tilts suggests that most of the observers' responses are actually based on the apparent tilt of the target, and not that of the flankers. These frequencies (Table 1) are no higher than those obtained with other perfectly obvious forced choices in our laboratory (e.g., Solomon, 2007), suggesting stimulus-independent causes of these "finger errors."[2]

Experiment 1

Estimates of orientation bias obtained with our unscaled stimuli appear in Figure 2. All biases were small at the fovea, and the noise had no obvious effect. With

	Fovea	Parafovea	Periphery
Noise absent E1	0.03%	1.64%	1.94%
Noise present E1	1.17%	1.64%	2.68%
Noise absent E2	1.02%	1.11%	1.99%
Noise present E2	2.60%	1.71%	1.12%
Noise absent E3		1.20%	0.76%

Table 1. Lapse rate (proportion of finger errors) at the tails of the psychometric function, pooled across observers and different flanker tilts at the three eccentricities tested. Top two rows are from Experiment 1 (E1) when stimuli were not embedded in noise (topmost row) or were embedded in noise (second row), bottom two rows are from Experiment 2 (E2) without noise (third from top) and in noise (bottom), last row is from Experiment 3 pooled across 2 spacings (Parafovea) or 3 spacings (Periphery).

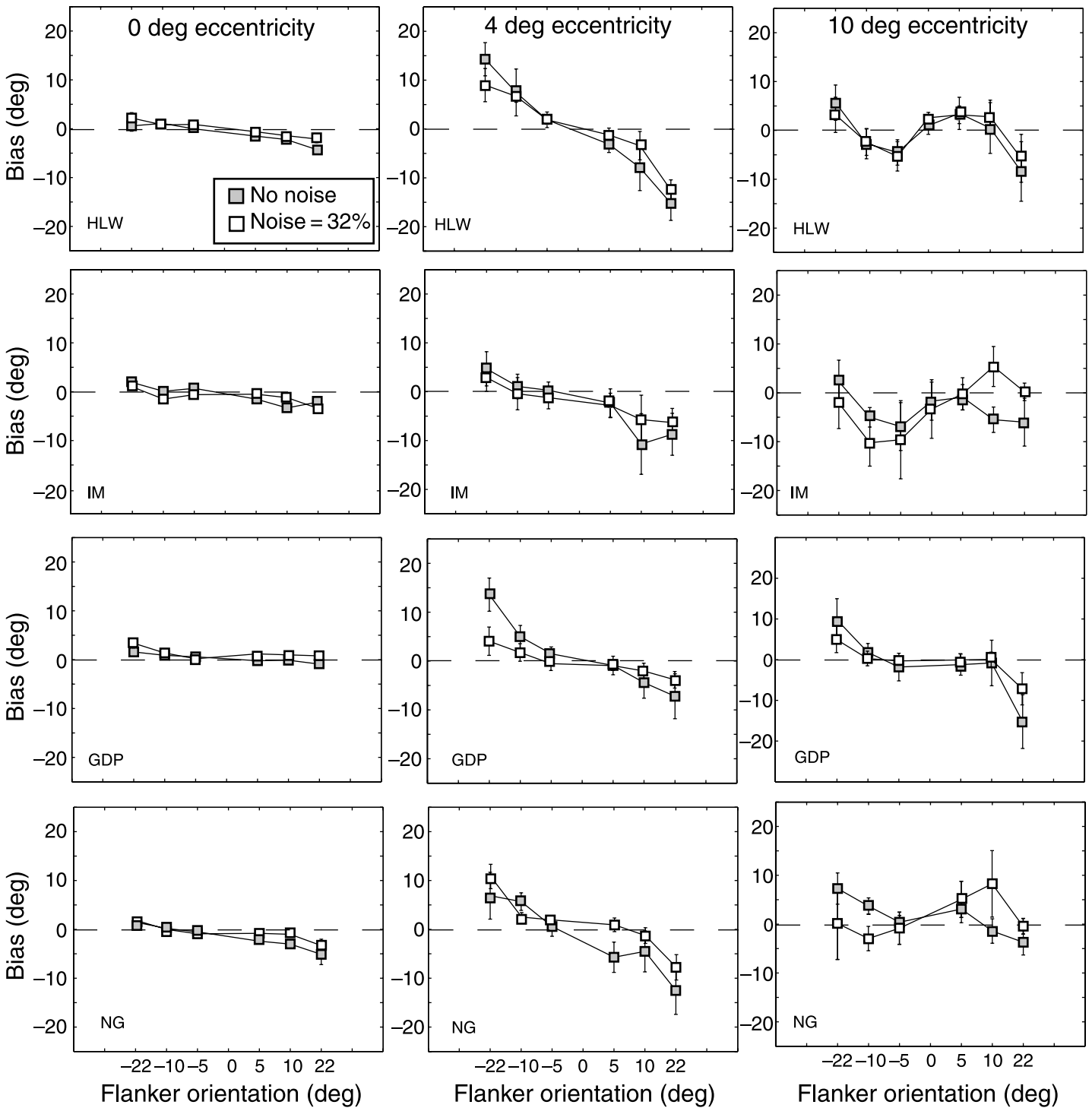

Figure 2. Orientation biases for flanked, unscaled targets in 32% noise (open symbols) and without noise (filled symbols). Each row shows data from a different observer. Each column shows data from a different retinal eccentricity. Error bars contain 2 standard deviations. Assimilation is indicated whenever biases have the same sign as the inducing flankers. Opposite signs indicate the tilt illusion.

parafoveal stimuli, on the other hand, we found two effects. First, the tilt illusion was often quite large, particularly with the ±22° flankers. Second, the repulsive biases measured in the presence of noise were smaller than those measured in the absence of noise. It is only with the peripheral stimuli that we obtained same-sign biases indicative of small-angle assimilation.

With these unscaled stimuli, the size of the tilt illusion varied non-monotonically with eccentricity: first increasing, then decreasing as the targets moved further into the

periphery. This non-monotonicity can be more easily appreciated by examining Figure 3, where the data from Figure 2 have been replotted as a function of eccentricity. We were not particularly interested in whether biases were clockwise or anti-clockwise *per se*, but rather whether they were assimilative or repulsive. Therefore, we flipped the sign of the biases that we measured with anti-clockwise flankers and pooled them with the biases that we measured with the corresponding clockwise flankers. The first four plots show the means of each observer's biases. The final plot shows the means of these means, after weighting the latter by the reciprocal of their standard errors.

All of these plots contain V-shaped curves, signifying more repulsion at 4° than at 0 or 10°.[3] In some cases (NG ± 5, IM ± 5, HLW ± 5, and HLW ± 10), the rightmost point of the V falls above the dashed line, indicating small-angle assimilation. In no cases, however, does the leftmost point fall above the dashed line. Thus, simply moving a stimulus into the periphery can change repulsion (i.e., the tilt illusion) into small-angle assimilation (and thus crowding). A similar finding was reported in the motion domain by Murakami and Shimojo (1993), who reported a switch from induced motion to motion capture that depended on viewing eccentricity.

Figure 4 plots biases measured when the stimuli were embedded in noise for the same observers. Although these curves are similar to those in Figure 3, most of the points here indicate greater (i.e., less repulsive/more assimilative) biases[4]. This can be seen even more clearly in Figure 5, where differential bias (i.e., bias in noise minus bias without noise) is plotted as a function of eccentricity. The addition of noise seems to have had little effect on the appearance of foveated stimuli and stimuli surrounded by ±5° flankers, but when the same stimuli were viewed at 4° and 10° eccentricities, biases increased. This indicates that the target looked more like its flankers when noise was present. In particular, the peripheral stimuli that produced moderate small-angle assimilation in the absence of noise produce quite marked small-angle assimilation here, where their visibility has been reduced by the addition of random texture.

Experiment 2

Biases for M-scaled stimuli presented without noise are plotted in Figure 6. Although there does seem to be a trend toward greater repulsion with increasing eccentricity[5],

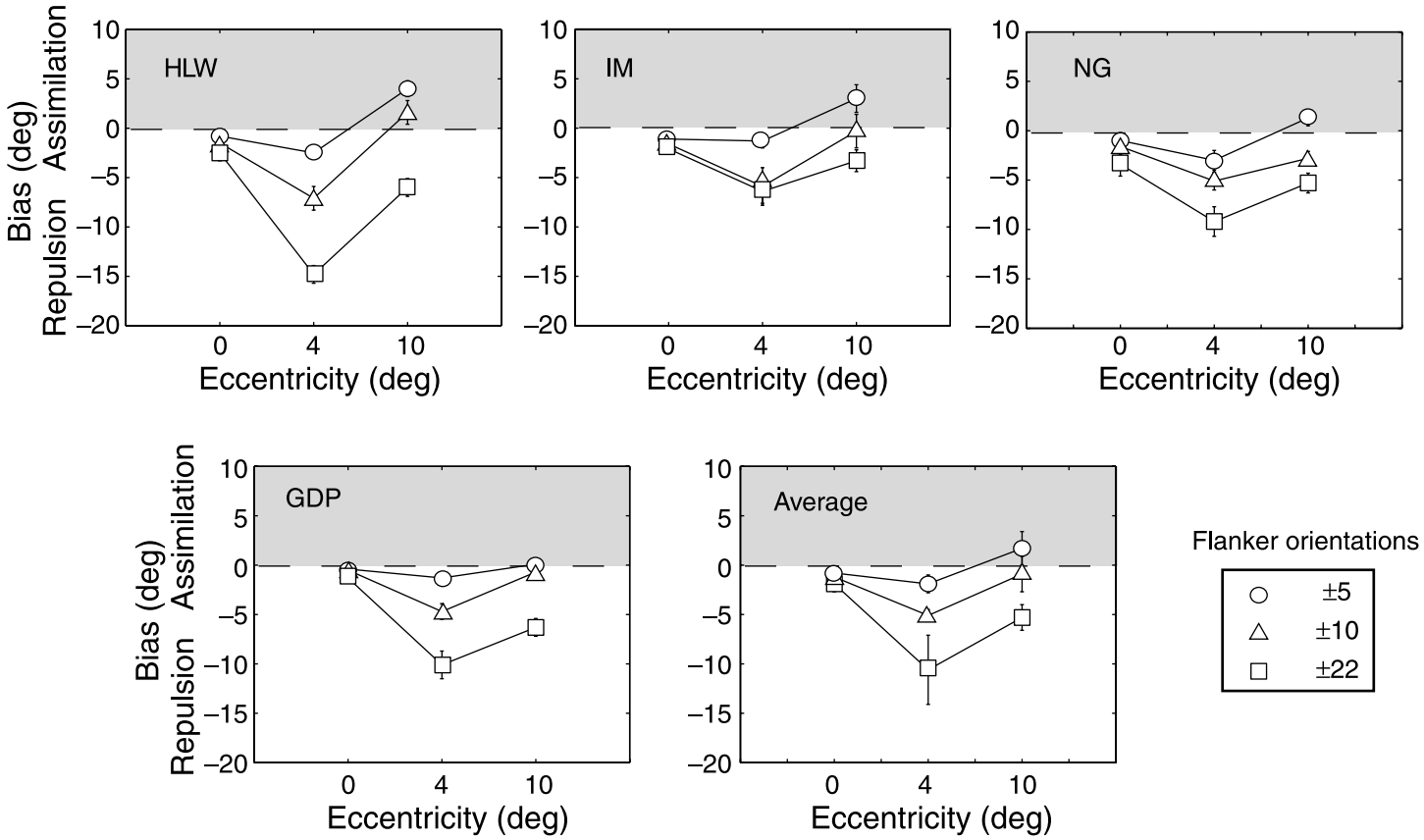

Figure 3. Orientation biases for flanked, unscaled targets without noise at the three eccentricities. Error bars contain two standard errors. The final plot shows the weighted averages of the four observers' biases. In this panel, error bars contain two average standard errors. (The same aforementioned weights were used when computing these latter averages.)

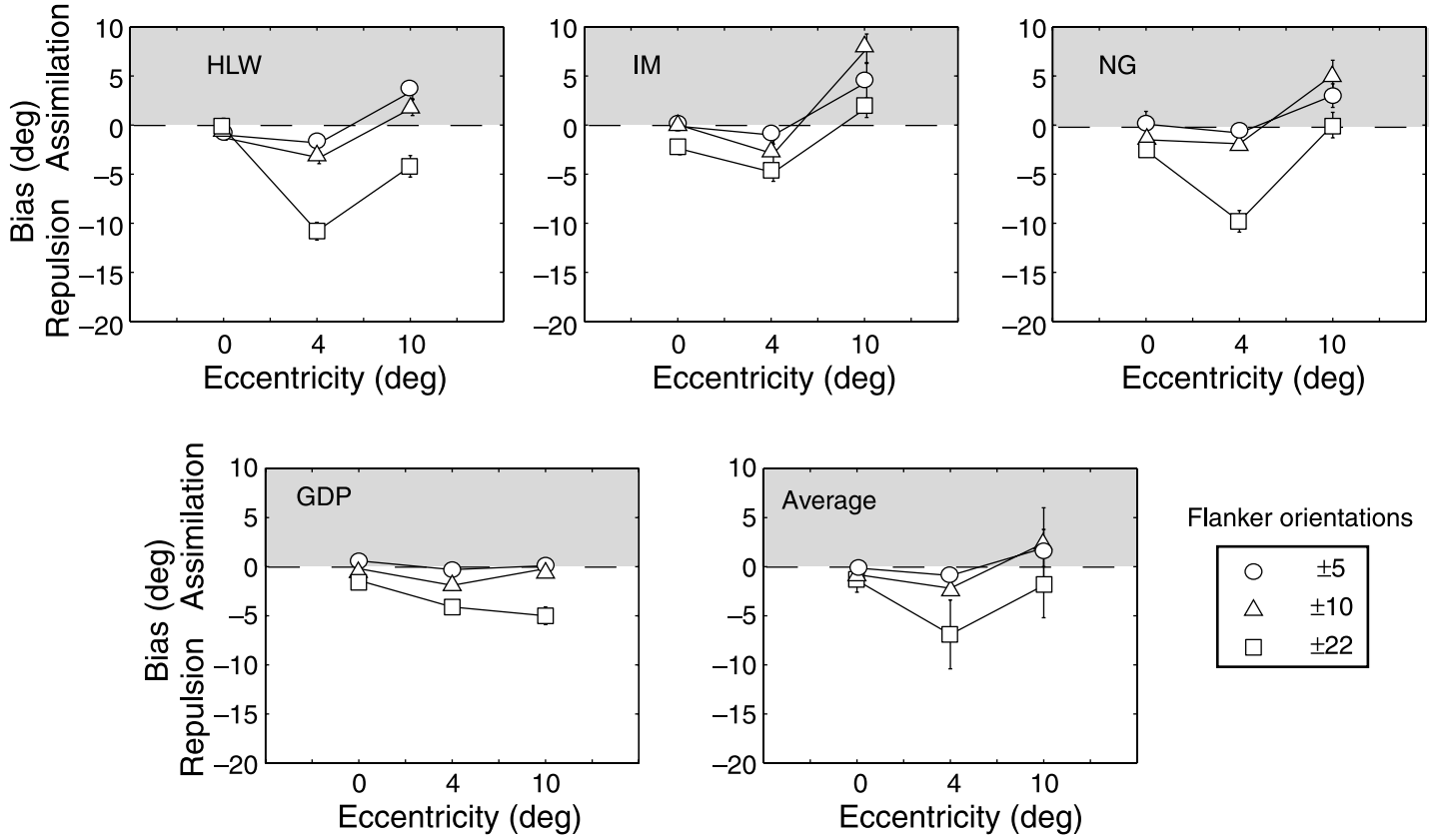

Figure 4. Orientation biases for flanked targets in noise. Layout identical to Figure 3.

these data do not exhibit the non-monotonicity seen in the results of Experiment 1. Indeed, these data do not contain any suggestion of assimilation. It is worth recalling that the stimuli presented at 4° eccentricity were very similar in the two experiments, while the foveal stimuli were much smaller and the peripheral stimuli were much larger in Experiment 2 than in Experiment 1. It appears that the result of our attempt to compensate for cortical coverage by M-scaling the stimuli is a severely attenuated effect of retinal eccentricity.

Biases for the same stimuli in noise are plotted in Figure 7. Similar to Experiment 1, the strength of repulsion is reduced by the addition of noise[6]. However, the addition of noise did not produce any assimilation in the periphery.

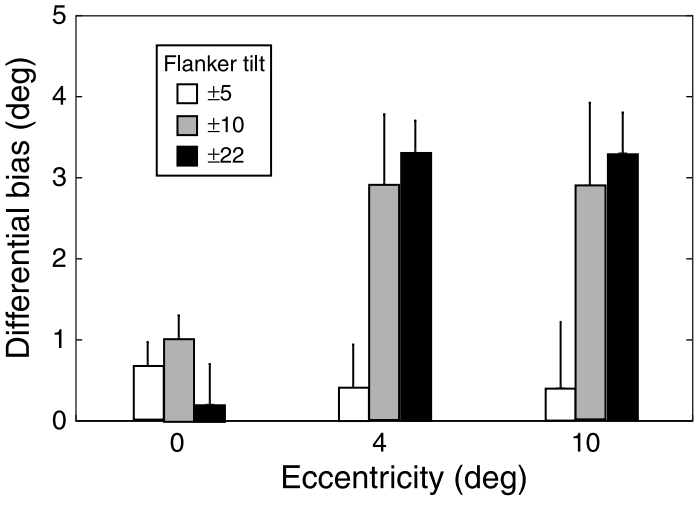

Figure 5. The effect of noise on orientation bias as a function of eccentricity. The differential bias (bias for stimuli in noise minus bias for noiseless stimuli) increases in size with eccentricity. Error bars are 1 *SEM*.

Experiment 3

If Equation 1 may be used as an index of the cortical distance between stimuli having the same retinal azimuth, then the smallest cortical distance between target and flankers used in the previous two experiments was when the target appeared at 10° eccentricity and the flankers were 1.75° away. These viewing conditions also produced our most compelling evidence for small-angle assimilation. If cortical proximity were all that was required for small-angle assimilation, then we should be able to establish evidence of it, even with targets at 4° eccentricity, provided the flankers are close enough. Similarly,

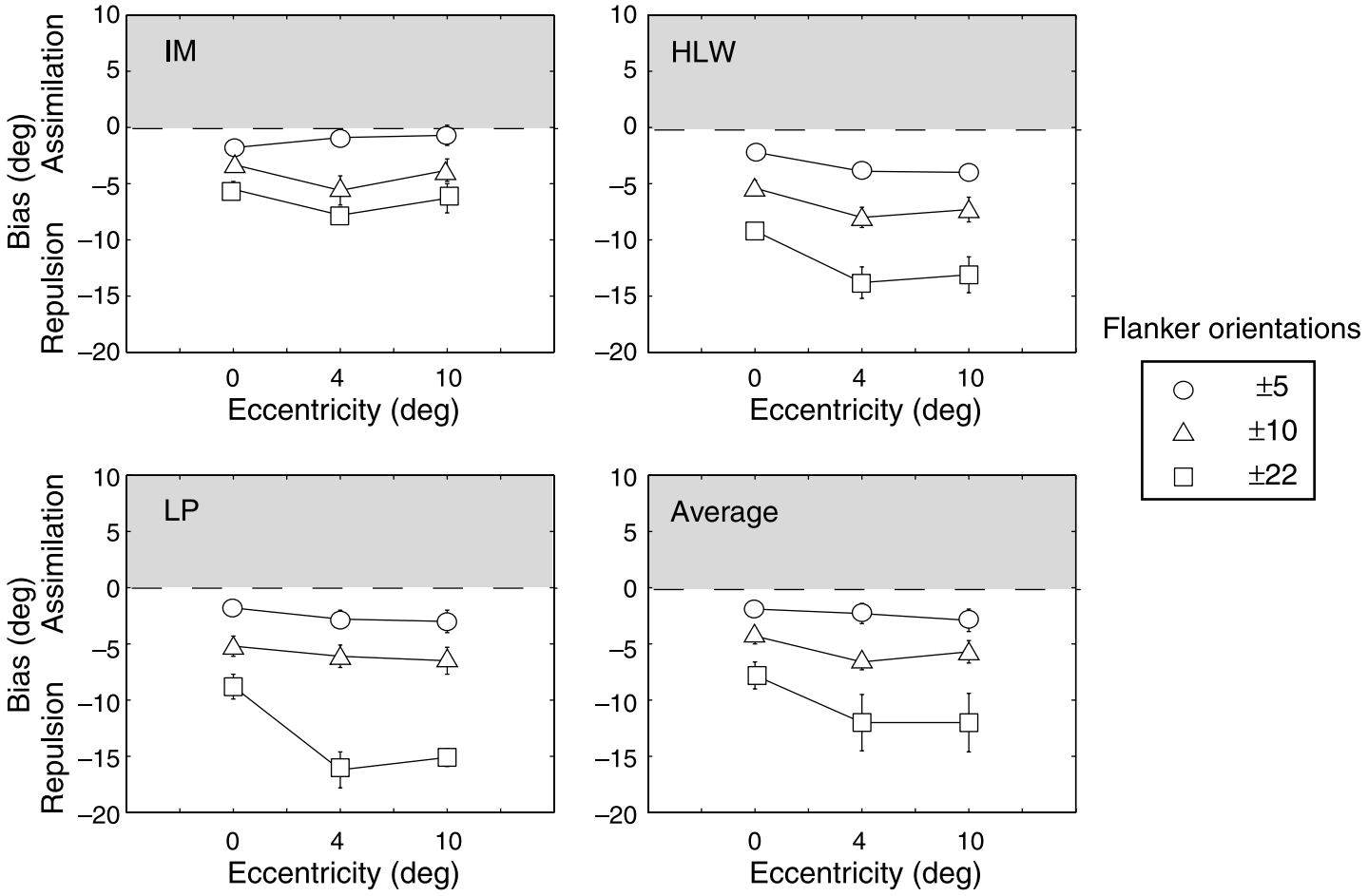

Figure 6. Orientation biases for scaled flanked targets. Layout identical to Figure 3.

we should be able to eliminate small-angle assimilation at 10° eccentricity, even without M-scaling. Simply moving the flankers further away should suffice. These were the goals of Experiment 3.

It can be seen in Figure 8 that both of these goals were achieved. Small-angle assimilation was obtained with targets at 4° eccentricity when their separation from the ±5° flankers was reduced to 1.19°, and repulsion was obtained with targets at 10° eccentricity when their separation from the ±5° flankers was increased to 3.17°. Also noteworthy are the results obtained with ±22° flankers. When they are too close to our peripheral target, the tilt illusion is reduced. Maximum repulsion occurs at an intermediate target–flanker separation.

Discussion

Experiment 1

The increase in bias (i.e., more assimilation, less repulsion) with decreasing signal-to-noise ratio suggests that, as visibility declines, information about orientation is pooled over increasingly large regions of the visual field. The addition of noise can also cause contextual assimilations of motion (Hanada, 2004) and shape (van der Kooij & te Pas, 2009). Kelly (1971) made an analogous observation regarding photoreceptors. When retinal illuminance was low, they integrated input over longer periods of time. Similarly in the spatial domain, when stimuli were presented at low contrast, observers integrated over a larger spatial extent (Tadin, Lappin, Gilroy, & Blake, 2003). Elsewhere (Morgan & Solomon, 2005; Parkes, Lund, Angelucci, Solomon, & Morgan, 2001) evidence has been presented that observers can be forced to pool orientation information across space, when given just a brief glimpse of a cluttered stimulus.

Pooling can be disadvantageous because it obscures genuine differences between visual signals. However, the visual system cannot represent signals with infinite fidelity, and there can be no advantage in preserving the noise with which the visual system corrupts its signals. Therefore, pooling can also be advantageous because independent samples of visual noise tend to cancel one another out. Since the visual system has fewer resources available for increasingly eccentric stimuli, we suspect that such stimuli

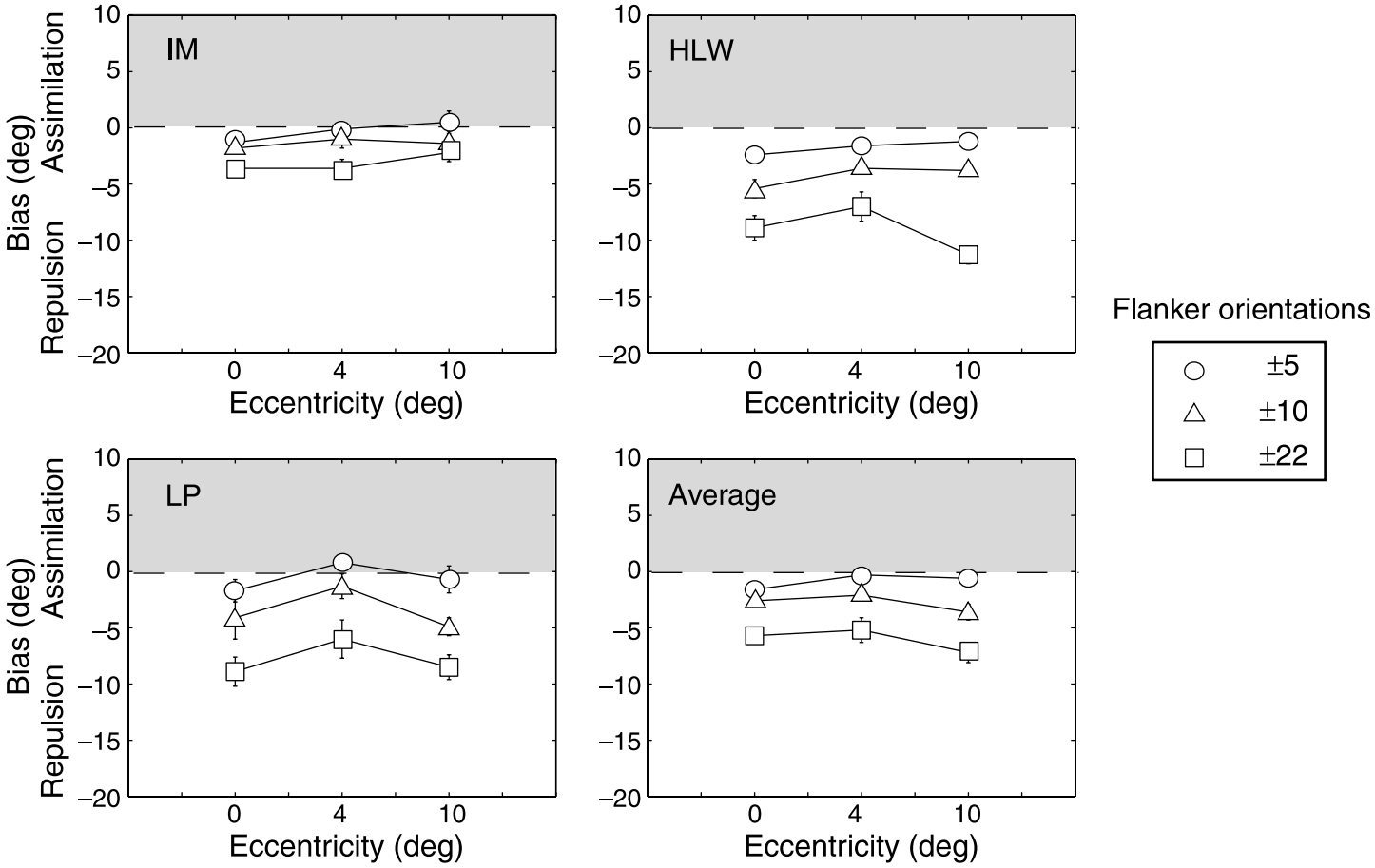

Figure 7. Orientation biases for scaled flanked targets in noise.

are represented with decreasing fidelity, and consequently the need for pooling increases.

The ubiquity of feature repulsions (e.g., the tilt illusion, simultaneous contrast, etc.) suggests that the advantages of exaggerating genuine differences between neighboring visual signals typically outweighs the need for squelching spurious differences introduced by visual noise (intrinsic and otherwise). Today (cf. Gibson, 1937), the most popular models of feature repulsion are based on the concept of gain control. A "canonical circuit" (Kouh & Poggio, 2008), which achieves gain control through divisive normalization, is thought to pervade the neural architecture at every level of processing.

Gain-control models suggest that feature repulsion should depend on the spread of divisive inhibition. When the cortical distance between target and flankers is small, we expect strong repulsion; when it is large, we expect weak repulsion. Of course, feature repulsion and feature pooling have opposite influences on orientation bias. If both of these influences depend on the cortical distance between target and flanker, then the results of Experiment 1 suggest that pooling outweighs repulsion only when the cortical distance between target and flanker is relatively small. That is because we found evidence of feature pooling (i.e., small-angle assimilation) only with the greatest retinal eccentricities, and consequently the least cortical coverage.

Experiment 2

M-scaling resulted in larger peripheral stimuli than those in Experiment 1. Consequently, the separation between target and flankers increased. Therefore, our failure to document any small-angle assimilation in Experiment 2 is not inconsistent with the notion that feature pooling operates over a much smaller region of cortex than the lateral inhibition putatively responsible for the tilt illusion. We should note that by scaling the stimuli, a number of features are necessarily changed in addition to target–flanker spacing. The difference in spatial frequency between the stimuli presented in the periphery was quite small (1.78 c/deg in Experiment 1 and 0.94 c/deg in Experiment 2) and as such unlikely to underlie the 7°–8° difference in biases between the two experiments. Size itself (rather than the size of the spaces between target and flanker) may also have had an effect on our results. However, Tripathy and Cavanagh (2002) and Pelli, Palomares, and Majaj (2004) report that the size of

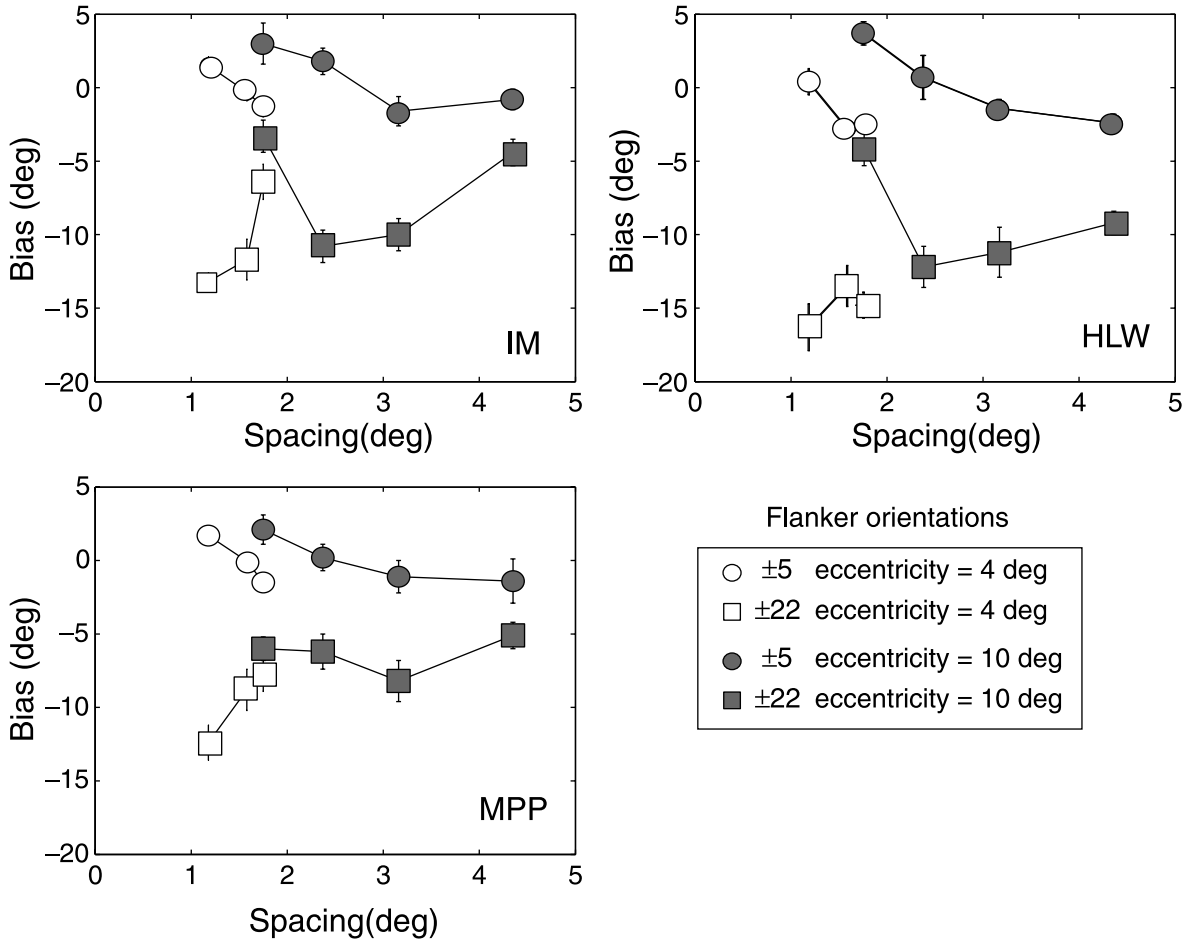

Figure 8. Biases measured in three observers as a function of target–flanker spacing, for stimuli presented at 4° eccentricity (open symbols) and at 10° eccentricity (filled symbols).

stimulus does not change the critical region for crowding. They report that the critical parameter underlying crowding is spacing, not size (see also Pelli & Tillman, 2008).

Experiment 3

Results from Experiment 3 underscore the importance of spacing on small-angle assimilation and the tilt illusion. The separation between target and flankers required for small-angle assimilation was found to increase with the target's eccentricity. Our results also suggest that the maximum tilt illusion is not always obtained when flanks abut the target (cf. Durant & Clifford, 2006; Tolhurst & Thompson, 1975; Wenderoth & Johnstone, 1988; all of whom investigated spacing at the fovea). In the periphery, maximum repulsion was recorded when the flankers were separated from the target.

Model

We would like to suggest that cortical spacing is the critical factor in determining the strengths of the contextual influences on perceived orientation. Previously, Motter and Simoni (2007) suggested that the critical region for crowding may correspond to a constant cortical separation. Initial measurements of this critical region were done by Bouma (1970), whose "rule of thumb" is now known as "Bouma's Law" (Pelli & Tillman, 2008). If we accept Bouma's Law for the critical region, then Motter and Simoni's suggestion can be written as

$$M(0.5w) - M(w) = c, \tag{3}$$

where $M(w)$ is the cortical magnification factor (in millimeters) as a function of eccentricity w (in degrees), and c is a constant. If Equation 3 is to hold for all $w > 0$, then $M(w)$ has to be logarithmic.[7]

In order to be consistent with Bouma's Law, our model uses a logarithmic approximation to Duncan and Boynton's (2003) formula for our non-foveal stimuli:

$$M'(w) = \begin{cases} M(w) & w \le 4 \\ 5.72 - \log_{1.73}(w) & w \ge 4 \end{cases}. \tag{4}$$

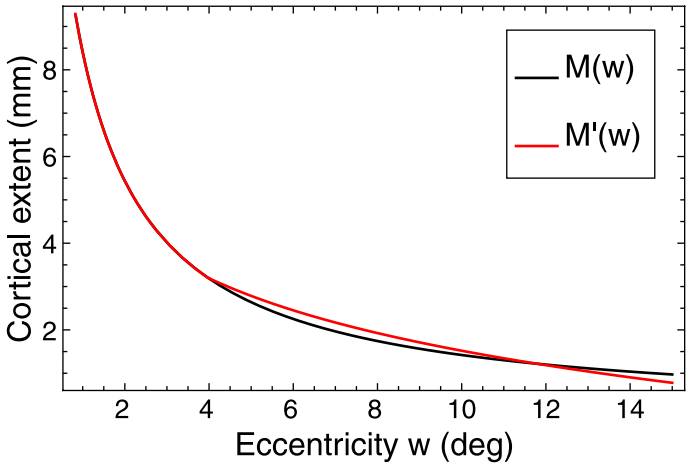

Figure 9. Graphical comparison between Duncan and Boynton's (2003) formula $M(w)$, and our approximation $M'(w)$, which is consistent with Bouma's Law (Equation 3), when $w \geq 4$.

A graphical comparison between Duncan and Boynton's $M(w)$ and our $M'(w)$ is provided in Figure 9.

In our model, bias ($-\mu$, defined empirically in Equation 2) reflects the difference between an assimilative force and a repulsive force,[8] each of which varies in proportion to the difference between target and flank orientations $\Delta\theta$, and a decaying function of the cortical distance between the target and its nearest flanker. In its most successful form, our model can be expressed as

$$-\mu = \Delta\theta\left(M_{\text{ass}}\exp\left[-D^2/\left(2\sigma_{\text{ass}}^2\right)\right] - M_{\text{rep}}\exp\left[-\lambda_{\text{rep}}D\right]\right), \quad (5)$$

where D is the cortical distance and M_{ass}, σ_{ass}, M_{rep}, and λ_{rep} are potentially free parameters, but see below.

As described in Equation 5, our model has the assimilative force decaying as a Gaussian function of cortical distance and the repulsive force decaying as an exponential function. This is illustrated in Figure 10a. Preliminary simulations with an exponentially decaying assimilative force did not produce the rapid change, which can be seen in Figure 10b, from assimilation with 5-deg flankers separated from the target by about 15% of its eccentricity to repulsion with 5-deg flankers separated from the target by about 40% of its eccentricity. That is because exponential functions change most rapidly at their peak (here at $D = 0$). Gaussian functions change most rapidly away from their peak (i.e., when $D > 0$).

For the present purposes, we apply Equation 4 to the eccentricity of each target w_{target} and its most peripheral flanker w_{flank} to approximate these distances:

$$D = \left[M'\left(w_{\text{target}}\right) - M'\left(w_{\text{flank}}\right)\right](1 + k\Delta\theta). \quad (6)$$

In the rightmost factor of the preceding equation, $\Delta\theta$ is the (unsigned) orientation difference between the target and its flanks, and k is a small, positive constant. Inclusion of this factor was motivated by the existence of orientation columns: In small regions of visual cortex, the proximity of any two neurons tends to increase with the similarity of their orientation preferences (Hubel & Wiesel, 1974). From a functional standpoint, inclusion of this term effectively reduces the influence of more oblique flankers on orientation bias.

Some of the model parameters have natural constraints. For the decay, we can constrain all four of these parameters to the positive numbers: M_{ass}, σ_{ass}, M_{rep}, and λ_{rep}. The first of these parameters has a further constraint, stemming from the fact that assimilation can be no greater than 100% of the difference between target and flank orientations, i.e., $M_{\text{ass}} \leq 1$. One final constraint concerns the constant k. While it does not seem unreasonable to imagine any of the other four parameters changing with signal strength, it does not really make sense that the distance between orientation columns would also change. Therefore, when finding the best possible fit of the most general, yet sensible form of this model to our data, we allowed 9 parameters to vary freely: one value for k, plus 2 values for each of the other four parameters (one for noisy stimuli, the other for noise-free stimuli).

As noted above, our data suggest that the repulsive force must decay more slowly with cortical distance than the assimilative force. Also noted above is the evidence suggesting an increase in either the strength or the extent of the assimilative force or a decrease in either the strength or the extent of the repulsive force, when the signal-to-noise ratio decreases.

All of the data we collected are summarized by the open and solid symbols in Figure 10. We obtained 40 predictions from our model; one for each condition in Experiments 1–3, not counting repeats. The r.m.s. standard error of these 40 predictions was 1.3° when the most general form of the model (i.e., the one with 9 free parameters) is the maximum-likelihood fit to all the data.

In an attempt at parsimony, we obtained fits to several nested models (i.e., with fixed parameter values). Chi-square tests (see Appendix A) suggest that two of these were significantly inferior [$1 - \chi^2_{(1)}(-2\ln\Lambda) < 0.02$] to the more general (9-parameter) model. In one of these inferior fits, we fixed $k = 0$. In two others, we either forced the high-SNR and low-SNR values of M_{ass} to be the same or we forced the high-SNR and low-SNR values of σ_{ass} to be the same. On the other hand, two nested models were not significantly inferior. (Comparison of the generalized likelihood ratio with chi-square suggests $1 - \chi^2_{(1)}(-2\ln\Lambda) > 0.25$.) In one of these models, there was only one value for M_{rep} (i.e., the same for both signal-to-noise ratios). In the other, there was only one value for λ_{rep}. Either of these models would have been suitable for illustration in Figure 10. We selected the latter, simply because it produced a slightly better fit. When both M_{rep}

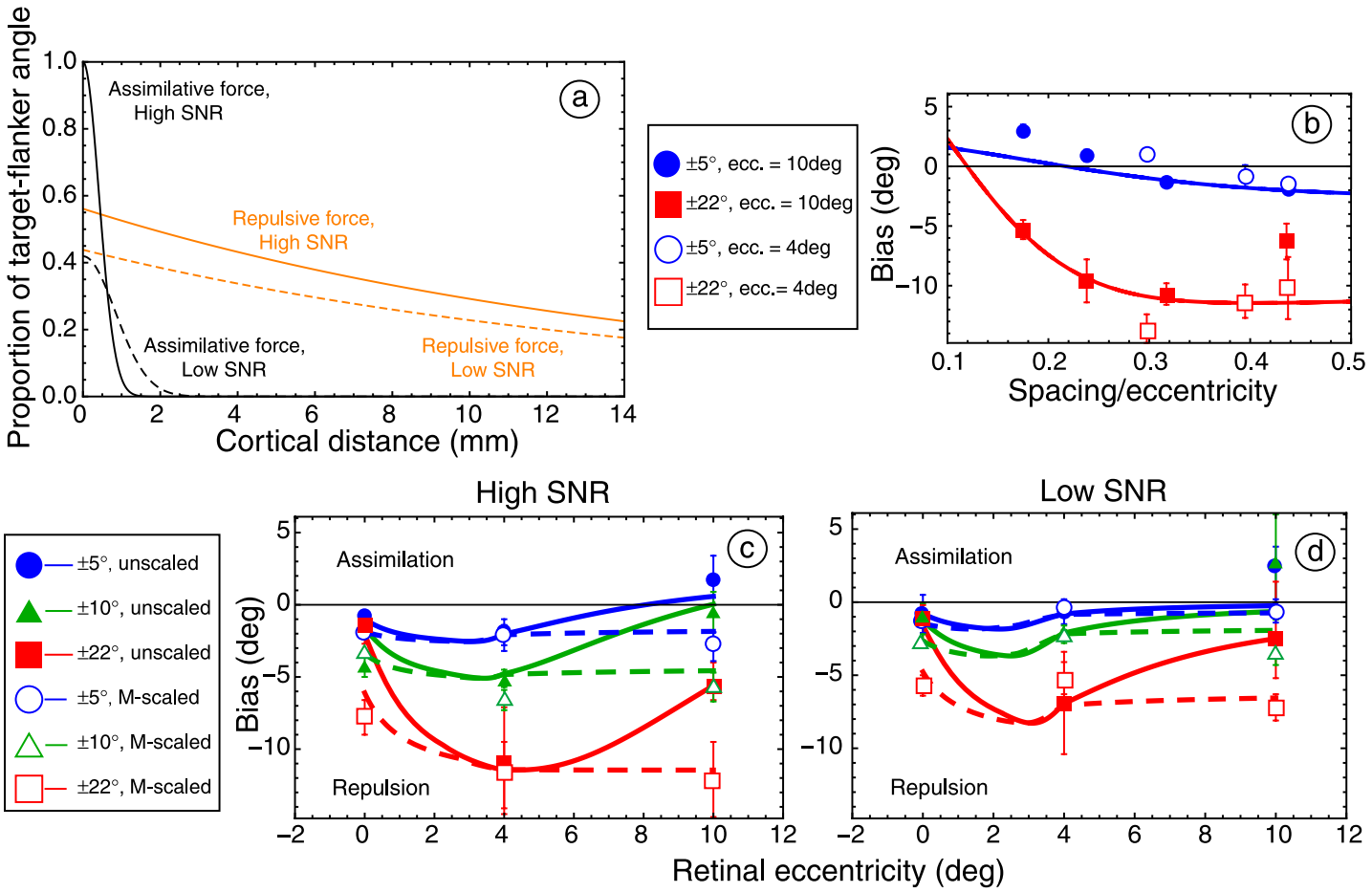

Figure 10. Average biases (symbols) and model fits (solid and dashed curves). (a) In the best-fitting model, the assimilative force A decays as a Gaussian function of cortical distance D. For low signal-to-noise ratios (SNR), $A = 0.42 \exp(-D^2/1.3)$; for high SNR, $A = \exp(-D^2/0.32)$. The repulsive force R decays as an exponential function of D. For low SNR, $R = 0.44 \exp(-0.065D)$; for high SNR, $R = 0.55 \exp(-0.065D)$. Model fits (curves in b–d) reflect the difference of these forces, multiplied by the difference between target and flanker angles. Panels (c) and (d) summarize Experiments 1 and 2; (b) summarizes Experiment 3. Error bars contain 2 standard errors.

and λ_{rep} were forced to remain invariant with SNR, the fit was significantly inferior.

Many aspects of the data are faithfully reproduced by the model, including the non-monotonic effect of eccentricity on the tilt illusion for unscaled stimuli, the reduced effect of eccentricity on M-scaled stimuli, and the switch from assimilation to repulsion with increased separation between the target and the ±5° flankers.

Following Murakami and Shimojo (1993), we have replotted all of our data in terms of the cortical distance between the target and its most eccentric flanker (see Figure 11). This allows readers to form an immediate appraisal of our suggestion that the cortical distance is what determines the influence flankers will have on a target's apparent orientation. When expressed as a fraction of flanker tilt, all our data form curves shaped like half the cross-section of a Mexican hat. Our model (the black curves) perhaps does not quite capture the rapidity with which assimilation changes to repulsion (at a cortical distance of approximately 0.5 mm), but otherwise it seems to fit the data rather well.

Conclusions

Two noteworthy results have arisen from these experiments. First, our results demonstrate that orientation biases increase (i.e., become more positive) when visibility is reduced. In the periphery, this increase can manifest as small-angle assimilation. Closer to the fovea, it manifests as a reduced tilt illusion. Our second noteworthy finding was the non-monotonic change in orientation bias with retinal eccentricity. This non-monotonicity was most evident with our unscaled stimuli. We attribute its cause to

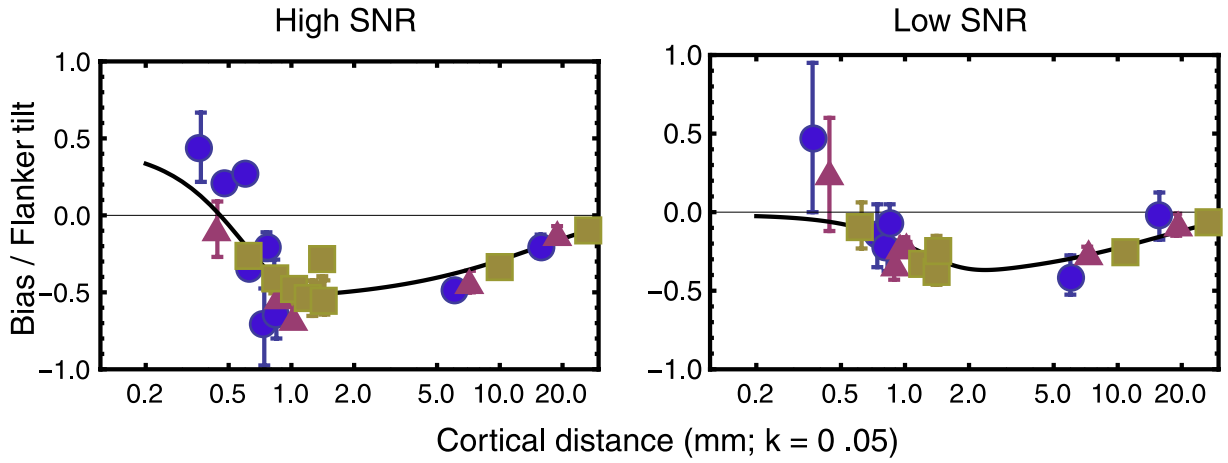

Figure 11. Average biases (symbols) and model fits (curves). We have modeled orientation bias as a fraction of flanker tilt (i.e., the orientation difference between target and flankers) that depends solely on the cortical distance between target and flanker (see Equation 5). All of our data with ±5° flankers (blue circles), ±10° flankers (purple triangles), and ±22° flankers (yellow boxes) can be seen to conform pretty well with this prediction. Note that our model fits best when ±22° flankers have a greater cortical distance from the approximately 0° target than ±5° flankers at the same retinal position. This effect of orientation columns is quantified by the parameter *k*.

opponent assimilative and repulsive forces, each of which has finite and unequal cortical extents. Because a great deal of cortex is devoted to the fovea, fixation of our target forced its flankers to the edge of the repulsive force's reach. As observers looked away from this target, its cortical coverage diminished, and the full weight of the repulsive force was manifest in our parafoveal measurements. However, as the observers looked even further away, the flankers became subject to an assimilative force, which dominates over relatively small cortical distances. Similar center–surround antagonism has been demonstrated at several levels of visual processing. To our knowledge, this paper is the first to suggest that the contextual influences on orientation perception behave in a similar manner.

Appendix A

If each set of measurements $\{x_{i,1}, x_{i,2}, \ldots, x_{i,Ni}\}$ is a sample from Gaussian distribution i, then we can estimate the likelihood of all measurements λ, given any predicted set of predicted values $\{p_1, p_2, \ldots, p_M\}$:

$$\lambda = \prod_{i=1}^{M}\prod_{j=1}^{N_i}\phi\left(\frac{p_i - x_{i,j}}{SD_i}\right), \tag{A1}$$

where ϕ denotes the standard normal probability density function. The log likelihood is thus

$$\ln\lambda = \sum_{i=1}^{M}\left(N_i \ln\frac{1}{\sqrt{2\pi}} - \sum_{j=1}^{N_i}\frac{\left[\left(p_i - x_{i,j}\right)/SD_i\right]^2}{2}\right). \tag{A2}$$

For convenience, we adopt the following notation for the squared average standard error of each prediction p_i:

$$SSE_i = \left[\frac{\sum_{j=1}^{N_i}\left(p_i - x_{i,j}\right)/N_i}{SD_i/\sqrt{N_i}}\right]^2. \tag{A3}$$

Thus

$$\ln\lambda = \sum_{i=1}^{M}\left(N_i \ln\frac{1}{\sqrt{2\pi}} - \frac{N_i}{2}SSE_i\right). \tag{A4}$$

Note that likelihood is maximized when total number of squared standard errors $T = \sum_i N_i SSE_i$ is minimized.

Finally, let sup λ_0 and sup λ denote the maximum likelihoods for any two nested models. To determine whether the more general model fits significantly better, we can apply the chi-square test to their generalized likelihood ratio (see Mood, Graybill, & Boes, 1974, p. 440):

$$-2\ln\Lambda = -2(\ln\sup\lambda_0 - \ln\sup\lambda) = \Delta T, \tag{A5}$$

where ΔT is the difference between the two models' total numbers of squared standard errors when maximum likelihood fit to all of the measurements.

Acknowledgments

We would like to thank John Greenwood for telling us that he found only assimilation for stimuli presented at 15 degree eccentricity. This project received support

from a cognitive systems foresight grant: BBSRC GR/E000444/01.

Commercial relationships: none.
Corresponding author: Isabelle Mareschal.
Email: Isabelle.Mareschal.1@city.ac.uk.
Address: Department of Optometry and Visual Science, City University, London, EC1V OHB, UK.

Footnotes

[1]It should be noted that the converse is not true: a loss of orientation acuity does not necessarily imply small-angle assimilation (Solomon & Morgan, 2009).

[2]Responses based on flanker appearance should produce assimilative biases. We found strong assimilation only with noise in Experiment 1's peripheral condition. This condition did produce the highest lapse rate, but further analysis of these errors reveals that only 53% of these lapses were in the same direction as the flank tilt. Since there was no consistent direction in these errors, we can be confident the assimilation reported below actually stems from the appearance of the target.

[3]Repulsion was significantly larger at 4° than at 10° eccentricity for both the ±10° flankers [$t(3) = 5.61$, $p < 0.05$] and the ±22° flankers [$t(3) = 5$, $p < 0.05$].

[4]Biases were significantly less repulsive in noise for the ±10° flankers at 4° eccentricity [$t(3) = 13.2$, $p < 0.05$] and for the ±22° flankers at 10° eccentricity [$t(3) = 3.23$, $p < 0.05$].

[5]It is not significant. A two-way ANOVA reveals a significant main effect only for flanker angle [$F(2, 18) = 9.68$, $p < 0.002$].

[6]With the ±10° flankers there were significant reductions in bias at both 4° eccentricity [$t(2) = 39$, $p < 0.05$] and 10° eccentricity [$t(2) = 4.8$, $p < 0.05$].

[7]Motter and Simoni's failure to adopt a logarithmic form of $M(w)$ is manifest in their Figure 7. According to their model, the critical separation on the cortex is not a constant function of eccentricity.

[8]We must be very careful to discriminate between small-angle assimilation, which is a name given to measured biases (Howard, 1982), and the visual process that causes it. We refer to the latter as an "assimilative force." This appellation is consistent not only with compulsory pooling, but other potential mechanisms as well. Although the term "feature repulsion" is similarly agnostic with regard to mechanism, we prefer "repulsive force," because it more obviously works in opposition to the assimilative force.

References

Brainard, D. H. (1997). The psychophysics toolbox. *Spatial Vision, 10,* 433–436.

Bouma, H. (1970). Interaction effects in parafoveal letter recognition. *Nature, 226,* 177–178.

Duncan, R. O., & Boynton, G. M. (2003). Cortical magnification within primary visual cortex correlates with acuity thresholds. *Neuron, 38,* 659–671.

Durant, S., & Clifford, C. W. G. (2006). Dynamics of the influence of segmentation cues on orientation perception. *Vision Research, 46,* 2934–2940.

Fritsches, K. A., & Rosa, M. G. (1996). Visuotopic organization of striate cortex in the marmoset monkey (*Callithrix jacchus*). *Journal of Comparative Neurology, 372,* 264–282.

Gibson, J. J. (1937). Adaptation, after-effect, and contrast in the perception of tilted lines. *Journal of Experimental Psychology, 20,* 553–569.

Hanada, M. (2004). Effects of the noise level on induced motion. *Vision Research, 44,* 1757–1763.

Howard, I. P. (1982). *Human visual orientation*. New York: John Wiley.

Hubel, D. H., & Wiesel, T. N. (1974). Sequence regularity and orientation columns in the monkey striate cortex. *Journal of Comparative Neurology, 158,* 267–293.

Jacobs, R. J. (1979). Visual resolution and contour interaction in the fovea and periphery. *Vision Research, 19,* 1187–1196.

Kapadia, M. K., Westheimer, G., & Gilbert, C. D. (2000). Spatial distribution of contextual interactions in primary visual cortex and in visual perception. *Journal of Neurophysiology, 84,* 2048–2062.

Kelly, D. H. (1971). Theory of flicker and transient responses: I. Uniform fields. *Journal of the Optical Society of America, 61,* 537–547.

Kouh, M., & Poggio, T. (2008). A canonical neural circuit for cortical nonlinear operations. *Neural Computation, 20,* 1427–1451.

Levi, D. M., Klein, S. A., & Aitsebaomo, A. P. (1985). Vernier acuity, crowding and cortical magnification. *Vision Research, 25,* 963–977.

Mood, A. M., Graybill, F. A., & Boes, D. C. (1974). *Introduction to the theory of statistics*. New York, USA: McGraw-Hill.

Morgan, M. J., & Solomon, J. A. (2005). Capacity limits for spatial discrimination. In L. Itti, G. Rees, & J. Tsotsos (Eds.), *Neurobiology of attention* (pp. 8–10). London: Elsevier.

Motter, B. C., & Simoni, D. A. (2007). The roles of cortical image separation and size in active visual search performance. *Journal of Vision, 7*(2):6, 1–15, http://www.journalofvision.org/content/7/2/6, doi:10.1167/7.2.6. [PubMed] [Article]

Murakami, I., & Shimojo, S. (1993). Motion capture changes to induced motion at higher luminance contrasts, smaller eccentricities, and larger inducer sizes. *Vision Research, 15,* 2091–2107.

Over, R., Broerse, J., & Crassini, B. (1972). Orientation illusion and masking in central and peripheral vision. *Journal of Experimental Psychology, 96,* 25–31.

Parkes, L., Lund, J., Angelucci, A., Solomon, J. A., & Morgan, M. (2001). Compulsory averaging or crowded orientation signals in human vision. *Nature Neuroscience, 4,* 739–744.

Pelli, D., Palomares, M., & Majaj, N. J. (2004). Crowding is unlike ordinary masking: Distinguishing feature integration from detection. *Journal of Vision, 4*(12):12, 1136–1169, http://www.journalofvision.org/content/4/12/12, doi:10.1167/4.12.12. [PubMed] [Article]

Pelli, D., & Tillman, K. A. (2008). The uncrowded window of object recognition. *Nature Neuroscience, 11,* 1129–1135.

Rovamo, J., & Virsu, V. (1984). Isotropy of cortical magnification and topography of striate cortex. *Vision Research, 24,* 283–286.

Solomon, J. A. (2007). Contrast discrimination: Second responses reveal the relationship between the mean and variance of visual signals. *Vision Research, 47,* 3247–3258.

Solomon, J. A., Felisberti, F., & Morgan, M. J. (2004). Crowding and the tilt illusion: Toward a unified account. *Journal of Vision, 4*(6):9, 500–508, http://www.journalofvision.org/content/4/6/9, doi:10.1167/4.6.9. [PubMed] [Article]

Solomon, J. A., & Morgan, M. J. (2006). Stochastic recalibration. *Proceedings of the Royal Society B, 273,* 2681–2686.

Solomon, J. A., & Morgan, M. J. (2009). Strong tilt illusions always reduce orientation acuity. *Vision Research, 49,* 819–824.

Stuart, J. A., & Burian, H. M. (1962). A study of separation difficulty: Its relationship to visual acuity in normal and amblyopic eyes. *American Journal of Ophthalmology, 53,* 471–477.

Tadin, D., Lappin, J. S., Gilroy, L., & Blake, R. (2003). Perceptual consequences of center–surround antagonism in visual motion processing. *Nature, 381,* 312–315.

Tolhurst, D. J., & Thompson, P. G. (1975). Orientation illusions and after-effects: Inhibition between channels. *Vision Research, 15,* 967–972.

Tripathy, S. P., & Cavanagh, P. (2002). The extent of crowding in peripheral vision does not scale with target size. *Vision Research, 42,* 2357–2369.

van der Kooij, K., & te Pas, S. F. (2009). Uncertainty reveals surround modulation of shape. *Journal of Vision, 9*(3):15, 1–8, http://www.journalofvision.org/content/9/3/15, doi:10.1167/9.3.15. [PubMed] [Article]

Wenderoth, P., & Johnstone, S. (1988). The different mechanisms of the direct and indirect tilt illusions. *Vision Research, 28,* 301–312.